AMERICAN PSYCHOLOGICAL ASSOCIATION

Journal of Experimental Psychology: General

ISSN: 0096-3445

2023, Vol. 152, No. 8, 2331–2344
https://doi.org/10.1037/xge0001404

Adaptation to Walking Direction in Biological Motion

Chang Chen[1], W. Paul Boyce[1], Colin J. Palmer[1, 2], and Colin W. G. Clifford[1]
[1] School of Psychology, University of New South Wales
[2] Department of Psychology, National University of Singapore

The direction that we see another person walking provides us with an important cue to their intentions, but little is known about how the brain encodes walking direction across a neuronal population. The current study used an adaptation technique to investigate the sensory coding of perceived walking direction. We measured perceived walking direction of point-light stimuli before and after adaptation, and found that adaptation to a specific walking direction resulted in repulsive perceptual aftereffects. The magnitude of these aftereffects was tuned to the walking direction of the adaptor relative to the test, with local repulsion of perceived walking direction for test stimuli oriented on either side of the adapted walking direction. The specific tuning profiles that we observed are well explained by a population-coding model, in which perceived walking direction is coded in terms of the relative activity across a bank of sensory channels with peak tuning distributed across the full 360° range of walking directions. Further experiments showed specificity in how horizontal (azimuth) walking direction is coded when moving away from the observer compared to when moving toward the observer. Moreover, there was clear specificity in these perceptual aftereffects for walking direction compared to a nonbiological form of 3D motion (a rotating sphere). These results indicate the existence of neural mechanisms in the human visual system tuned to specific walking directions, provide insight into the number of sensory channels and how their responses are combined to encode walking direction, and demonstrate the specificity of adaptation to biological motion.

Public Significance Statement
Our ability to perceive walking direction has critical importance to social behavior. Here, we investigate how the walking direction of conspecifics is represented in the human visual system. Prolonged viewing of walking motion in one direction biases the perceived direction of subsequent motion—referred to as a perceptual aftereffect. By investigating the psychophysical constraints of this effect (including angular tuning and stimulus specificity), we report evidence for a population-coding model of perceived walking direction, comparable in its structure to the sensory coding of orientation or low-level motion direction in the visual cortex. Our results provide a basic computational framework for understanding how social information that is conveyed by biological patterns of motion (here, three-dimensional walking direction) is encoded in the visual system.

Keywords: visual aftereffect, point-light walker, social vision, person perception

Supplemental materials: https://doi.org/10.1037/xge0001404.supp

Characteristic patterns of motion produced by the human body can convey information critical to social behavior, including walking direction (Jackson & Blake, 2010; Theusner et al., 2011), gender (Cutting & Kozlowski, 1977; Pollick et al., 2005; Troje, 2002), identity (Cutting & Kozlowski, 1977; Troje et al., 2005), and emotional state (Dittrich et al., 1996; Montepare et al., 1987). Human observers

This article was published Online First March 23, 2023.
Chang Chen https://orcid.org/0000-0001-5083-698X
The authors presented part of this research (Experiments 1 and 2) as a poster at the 43rd European Conference on Visual Perception (ECVP) in August 2021.

This research was supported by Australian Research Council Discovery Projects DP200100003 to CJP & CWGC, DP160102239 to CWGC, and Australian Government Research Training Program Scholarship to CC.

Data, analysis scripts, and videos are available online at OSF site: https://osf.io/t8cdn/?view_only=4e3f19ba1060462995c1d5dbd5807bde

Chang Chen served as lead for data curation, formal analysis, project administration, and writing–original draft and served in a supporting role for software. W. Paul Boyce served as lead for software and served in a supporting role for conceptualization, data curation, formal analysis, methodology, project administration, resources, supervision, validation, and writing–review and editing. Colin J. Palmer served in a supporting role for conceptualization, formal analysis, funding acquisition, methodology, software, supervision, and writing–review and editing. Colin W. G. Clifford served as lead for funding acquisition, investigation, resources, supervision, validation, and writing–review and editing and served in a supporting role for formal analysis, project administration, and software. Chang Chen and Colin W. G. Clifford contributed equally to conceptualization, visualization, and methodology.

Correspondence concerning this article should be addressed to Chang Chen, School of Psychology, University of New South Wales, Mathews Building, Botany Street, Randwick, Sydney, NSW 2052, Australia. Email: chang.chen2@unsw.edu.au

readily discern such information even from animations that capture only the trajectory of key joints—referred to as point-light animations (Blake & Shiffrar, 2007; Johansson, 1973). Walking direction, for example, can be identified from point-light animations immersed in dynamic visual noise (Bertenthal & Pinto, 1994; Neri et al., 1998; Thornton et al., 1998; Thurman & Grossman, 2008) or presented peripherally (Thompson et al., 2007) and tends to be processed incidentally even when detrimental to the task at hand (Thornton & Vuong, 2004). That the perception of point-light walkers is severely impaired if presented upside down implicates specialized visual mechanisms for processing typical patterns of biological motion (Troje et al., 2006; Watson et al., 2004). There is an ongoing debate about the relative contribution of local versus global visual cues to biological motion perception, with evidence that walking direction can be signaled by local cues such as individual foot trajectories (Troje & Westhoff, 2006) as well as more holistic bodily form cues (e.g., Beintema et al., 2006).

How does the visual system code human motion to enable accurate and reliable interpretation of others' behavior in social environments? We address this question here using the technique of psychophysical adaptation. Adaptation is a fundamental characteristic of sensory processing associated not only with low-level features (e.g., color) but also with high-level attributes of faces and objects (e.g., eye gaze; Palmer & Clifford, 2017). Prolonged exposure to a stimulus can temporarily reduce the sensitivity of discrete neuronal populations tuned to the adapting stimulus and produce biases in perception. The adaptation paradigm is often referred to as the "psychologist's microelectrode" (Frisby & Stone, 2010) because it can be used to demonstrate that a given stimulus has a unique neuronal representation (Clifford et al., 2007; Mather et al., 2008). Previous studies have used adaptation techniques to explore neural processing in high-level vision, finding evidence for neurons selective for attributes such as face identity and gaze direction (Jenkins et al., 2006; Leopold et al., 2001). Adaptation to biological motion has been used to modulate gender perception (Jordan et al., 2006; Troje et al., 2006) and investigate how form, motion, and depth are processed when perceiving biological motion (Benton et al., 2016; Jackson & Blake, 2010; Theusner et al., 2011). Adaptation has also been used in neuroimaging studies to identify brain regions encoding attributes of biological motion, such as action-specific neural tuning in the human posterior superior temporal sulcus (Grossman et al., 2010; Thurman et al., 2016).

Adaptation to specific walking directions was first reported by Jiang and He (2008), namely a repulsive aftereffect whereby adaptation to walkers oriented left or right biased perception of walking direction in the opposite direction. Jackson and Blake (2010) extended these findings to three-dimensional representations of walking direction and demonstrated that perceptual aftereffects following adaptation to walking direction are robust to changes in size and retinal position. While such aftereffects indicate visual mechanisms tuned to specific walking directions, the functional architecture of this system remains unknown. Moreover, visual processing of biological motion remains largely unexplored across the full range of possible walking directions that we observe in everyday life, especially in three-dimensional environments.

In the current study, we employed point-light walker stimuli in an adaptation paradigm to measure the strength of aftereffects as a function of adapting direction (Experiment 1) and test direction (Experiment 2). To account for the resulting data, we propose a simple computational model in which information about walking direction is coded across a population of neurons tuned to different walking directions. This model incorporates principles of sensory coding that are well established in other areas of vision processing, namely population coding (Suzuki et al., 2005) and the normalization of sensory responses (Carandini & Heeger, 2012). Gain control via normalization offers a way to understand the functional role of sensory adaptation (Clifford & Rhodes, 2005). Models based on adaptive gain control have been applied to the processing of low-level visual attributes such as orientation, color, and local motion (Clifford et al., 2000) and, in social vision, to the coding of others' gaze direction (Palmer & Clifford, 2017). However, modeling biological motion adaptation in terms of sensory gain control remains largely unexplored. The current study examines whether this framework is useful for understanding how the visual system encodes the higher-level, socially relevant cue of perceived walking direction. This is motivated partly by the notion of "canonical" neural computations that are repeated in neural circuits across different levels of the visual system. For example, a divisive normalization is a specific form of sensory gain control that was proposed initially to account for neurophysiological responses in the primary visual cortex (e.g., Heeger, 1992), before being extended to understand aspects of sensory processing more widely (Carandini & Heeger, 2012). The population-coding model that we implement in the current study incorporates such response normalization and generates specific predictions for the tuning profile of perceptual aftereffects following adaptation to walking direction, which fit well with data observed in Experiments 1 and 2. These data also provide insight into the bandwidth and number of sensory channels involved in the sensory coding of walking direction.

To further elucidate how information about walking direction is coded in the visual system, Experiment 3 tested for specificity in how walking direction is coded in depth. In particular, we test whether adaptation to the horizontal component of walking direction (i.e., leftward vs. rightward walking direction) retains specificity to the walking direction in depth (i.e., walking toward the observer vs. walking away from the observer) or generalizes across the depth axis. This provides insight into how walking direction is coded across the full 360° range of possible walking directions that we observe in three-dimensional environments.

Experiment 4 investigated the specificity of adaptation to biological motion rather than generic three-dimensional representations of motion direction. While previous work indicates that adaptation to biological motion is unlikely to be explained by low-level adaptation in the visual system (e.g., because adaptation to walking direction persists across changes in size and retinal position between the adapting and test stimuli; Jackson & Blake, 2010), these effects might in principle reflect adaptation of neurons tuned generally to object-level motion direction rather than the direction of movement conveyed specifically by the human form. Experiment 4 addresses this question by testing whether adaptation to motion direction generalizes across point-light walker stimuli and a nonbiological form of 3D motion (a rolling sphere).

Experiment 1: Tuning of Aftereffects Across Different Adaptor Walking Directions

Experiment 1 was designed to measure the tuning of perceptual aftereffects across changes in the walking direction of the adapting

stimulus. Participants reported the walking direction of point-light walkers that varied in horizontal walking angle, and we measured how the stimulus angle perceived as walking directly toward the observer changed as a result of adaptation. We implement a population-coding model that accounts for the tuning of perceptual aftereffects in terms of the underlying sensory coding of walking direction across a neuronal population.

Method

Participants

Eight participants (five males, three females), including the four authors, took part in Experiment 1. The other four participants were naïve as to the purpose of the experiments. We did not have a strong expectation about effect size. The target sample size was set to 8 before data collection, based on sample sizes used in previous research on adaptation to directional cues in social vision (Jackson & Blake, 2010; Palmer & Clifford, 2017). The total test time for each participant was about 5 hr. All participants had a normal or corrected-to-normal vision. The study was approved by, and conducted in accordance with, the guidelines of the University of New South Wales Human Research Ethics Committee.

Apparatus and Stimuli

Stimulus presentation was controlled in MATLAB using Psychtoolbox (Brainard, 1997) on a Display++ LCD monitor (Cambridge Research Systems; 1,920 × 1,080-pixel resolution; 32-in.; 120 Hz refresh). Point-light animations of a human walker were shown in the middle of the screen as white dots (120 cd/m^2) on a black background at a viewing distance of 57 cm in a darkened room, such that 1 cm on-screen subtended 1° of visual angle at the observer and each pixel subtended 2.2 min of arc. Prototypical walking action was obtained from the Carnegie Mellon University (CMU) motion-capture database (http:/mocap.cs.cmu.edu) and displayed as point-light stimuli using the Biomotion Toolbox (van Boxtel & Lu, 2013). The number of dots on the body of each point-light walker was 41 in each frame of the animation, and the dots were anti-aliased circles set to 1-pixel diameter. The animation data in each point-light walker were a representation of where the joints were located over time in 3D space, and so could be rotated in 3D to precisely manipulate the horizontal walking angle relative to the viewer (Figure 1A).

Experimental Design

Experiment 1 used a repeated-measures design, with each condition measuring the effect of adaptation to a different walking direction. Each condition consisted of two phases: a baseline phase followed by an adaptation phase (Figure 2). In the baseline phase, participants were presented with a series of 60 trials in which they judged the walking direction of a test stimulus. The test stimuli were point-light walkers presented for 508 ms. The forced-choice task was to indicate the direction (left or right of directly toward the observer) in which each walker was heading by pressing one of two response buttons on the keyboard (left or right arrow). There was a gray fixation marker presented on the screen until a valid response was made. Following each response, there was a 500 ms interval before the next trial was initiated.

The horizontal walking direction of the test stimuli was varied by rotating the animation around the vertical axis. The direction of motion of the test stimuli varied from trial to trial under computer

Figure 1
Illustrations of Walker and Scrambled Stimuli

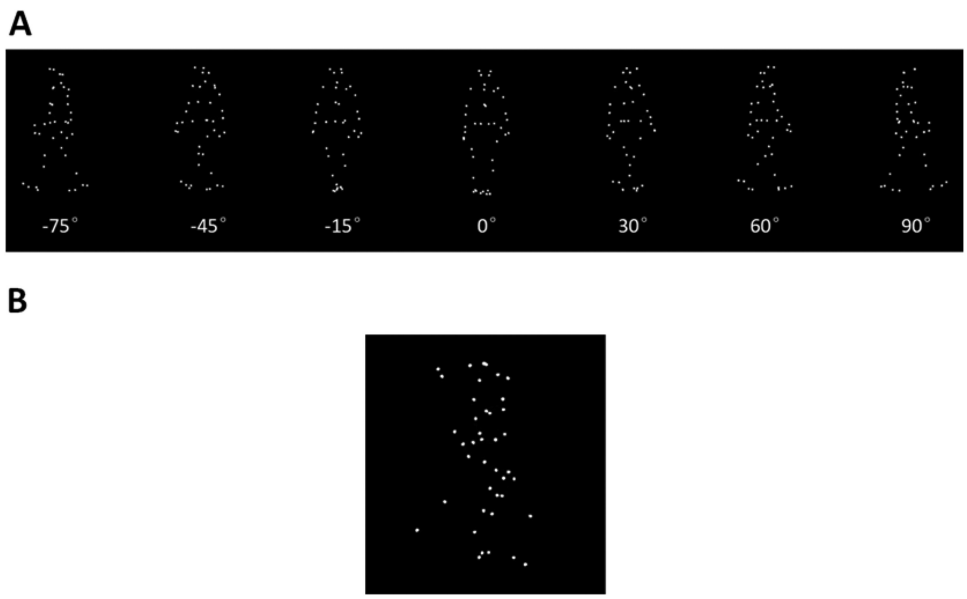

Note. (A) Examples of point-light walker stimuli with walking direction toward direct (0°), 30°, 60°, and 90° to the right, and 15°, 45°, and 75° to the left. (B) An example scrambled stimulus from Experiment 1 (Video 1 in the online supplemental material).

Figure 2
Schematic Illustration of Experimental Paradigm

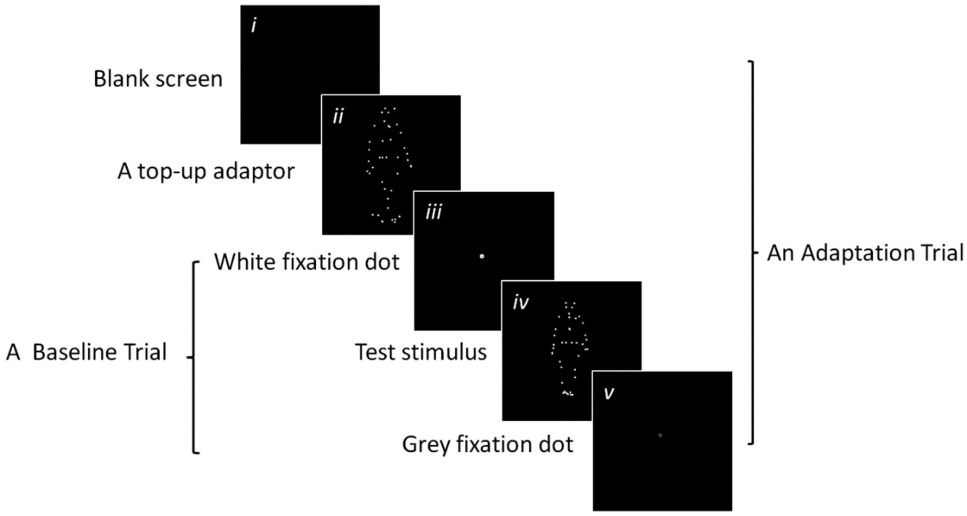

Note. In an adaptation trial, participants viewed: (i) a blank screen presented for 500 ms; (ii) a top-up adaptor presented for 4 s to maintain adaptation throughout the task; (iii) a white fixation dot presented for 750 ms; (iv) a test stimulus presented for 508 ms; (v) a gray fixation presented until response. In a baseline trial, participants viewed (iii)–(v).

control according to an adaptive staircase procedure ("Psi"; Kontsevich & Tyler, 1999), ranging from −15° (leftward) to +15° (rightward), with a precision of 0.1°. The adaptive staircase provided a measure of the point of subjective equality (PSE) and the error associated with that estimate. The PSE was the direction of the test stimulus at which the participant was likely to respond "left" or "right" with equal probability and provided a sensitive measure of the veridical direction of the test that was perceived as heading directly toward the viewer. In Experiment 1, we used two runs of the adaptive staircase within each phase of the task and then averaged the PSE between them.

For each condition, after completing the baseline phase, participants completed the adaptation phase. The adaptation phase was similar to the test phase, except that in each trial, participants viewed an adapting stimulus for 4 s before the presentation of the test stimulus. There was a white fixation point presented for 750 ms between each adaptor and test stimulus. In each condition, the adaptation stimulus was walking in a specific direction, for example, 45° rightward. This phase of the task also began with an initial adaptation period, in which eight adaptor stimuli (with a blank screen of 500 ms between each) were displayed consecutively for 4 s each (for a total duration of 32 s). After this initial adaptation, the instructions for the following task were presented on the screen and a key press was required to advance (to view an adaptation phase, see Video 2 in the online supplemental material).

The strength of adaptation was compared for 13 adapting walking directions in 15° intervals around 0° (toward), ranging from −90° (leftward) to +90° (rightward) as shown in Figure 1A. To ensure that adaptor and test stimuli had very different local motion properties, the height of the adaptor stimulus was 10° and the height of the test stimulus was 8°. To match the local, low-level motion properties of the walking stimulus while removing the spatiotemporal relationship between dots, another two adapting stimuli were presented in separate conditions as scrambled dots (Figure 1B). Each dot of a scrambled stimulus started at a random frame within each animation and all the scrambled stimuli were generated by spatially scrambling each dot of an intact walker from ±30° walkers (these directions were chosen as they produced the largest adaptation effects during piloting). The order of the 15 adaptation conditions (13 intact and two scrambled walkers) was randomized across participants. To allow the visual system to recover from the adaptation induced on the previous condition, there was at least a 10-min gap between the end of the adaptation phase of each condition and the beginning of the baseline phase of the next condition.

Psychophysical Modeling for Experiments 1 and 2

To quantify the aftereffect of adapting direction on perceived walking direction, we fit a model of the magnitude of the aftereffect as a function of the adapting direction (described in Figure 3).

Prior to adaptation, the unadapted response, R_u, of a population of hypothetical direction-selective neurons to a test walker moving in direction θ_t is modeled as a Gaussian function (G) of the difference between neuronal preferred direction, φ, and the test direction:

$$R_u(\vartheta_t, \varphi) = G(\vartheta_t - \varphi, \sigma^2) \quad (1)$$

where σ is the width of the excitatory response.

Adaptation is modeled as reducing neuronal gain in proportion to the response to the adapting stimulus, with constant of proportionality α. If the direction of the adapting stimulus is θ_a, then the adapted response, R_a, to a subsequent test stimulus in direction θ_t is given by:

$$R_a(\vartheta_t, \vartheta_a, \varphi) = G(\vartheta_t - \varphi, \sigma^2) * (1 - \propto^* G(\vartheta_a - \varphi, \ \sigma^2)) \quad (2)$$

The perceived direction of motion, P, is then modeled as the peak of the neuronal population response, that is, the preferred direction of

Figure 3
Schematic Illustration of the Model

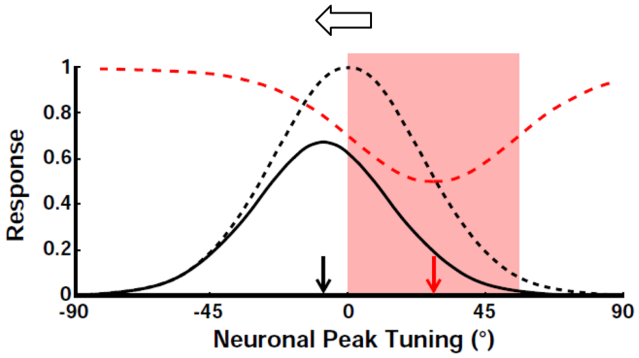

Note. Schematic illustration of the model of biological motion adaptation. The response of a hypothetical population of direction-selective neurons is shown as a function of the neuronal peak direction tuning. Prior to adaptation, the response to a test stimulus walking toward the observer (0°) is a hill of activity (dashed black line), centered on the test direction of 0°. The effect of adaptation to a 30° walker on the gain of the neurons responding to the test illustrated is to inhibit their activity in a direction-tuned manner (red dashed line), with the maximal inhibition (shaded red region) occurring around the direction adapted to (red arrow). The predicted population response (solid black line) to a 0° test stimulus subsequent to adaptation is obtained by multiplying the unmodulated population response (dashed black line) by the gain (dashed red line). The overall population response is reduced (compare area under response profiles) and biased away from the direction of the adapting stimulus (in the direction of the white arrow). Hence, the population codes a direction (black arrow) consistent with a repulsive aftereffect. The magnitude of the predicted shift in coded direction is maximal when adaptation affects the near flank of the hill (much) more than the far flank, as illustrated—hence, the model predicts that the magnitude of perceptual aftereffects will be tuned to the walking direction of the adaptor relative to the test stimulus. See the online article for the color version of this figure.

the neuron giving the maximum response:

$$P(\vartheta_t, \vartheta_a) = \max\left(R_a\left(\vartheta_t, \vartheta_a, \varphi\right)\right) \quad (3)$$

The aftereffect is then modeled as the difference between the adapted and unadapted perceived directions of motion.

The model was fit to the data by minimizing the error between model and response data using the *fminsearch* function in MATLAB, allowing two parameters to vary: α and σ.

Data Analysis

For all the experiments (Experiments 1–4), the initial data processing was performed using custom MATLAB scripts. And all the subsequent statistical analyses were conducted with IBM SPSS (Version 22) using one-way or two-way repeated-measures Analysis of Variance (ANOVA), one-sample tests, and paired samples *t*-tests where appropriate. *T*-tests with Holm–Bonferroni corrections were used where appropriate. When necessary, post hoc tests following ANOVA were conducted with Holm–Bonferroni correction. The threshold for statistical significance was set at 0.05 ($p < .05$). Greenhouse–Geisser corrections were used if the sphericity assumption was violated. Effect sizes were given as partial η^2.

Transparency and Openness

The choice of sample size is noted in the Participants section for each experiment reported in this article. All data exclusions, manipulations, and measures are reported. All data, analysis scripts, and experimental videos are available at https://osf.io/t8cdn/?view_only=4e3f19ba1060462995c1d5dbd5807bde. The experiments reported in this article were not preregistered.

Results

Overview of Data

Experiment 1 investigated the strength of the aftereffect of perceived walking direction as a function of adapting direction. The results in Figure 4 show the mean aftereffects across participants ($N = 8$). The aftereffect was computed as the difference between the adapted PSEs and the corresponding unadapted (baseline) PSEs, such that a positive aftereffect indicates an adapted PSE more rightward than the unadapted PSE; a negative aftereffect indicates an adapted PSE more leftward than the unadapted PSE. Note

Figure 4
Results of Mean Aftereffect in Experiment 1

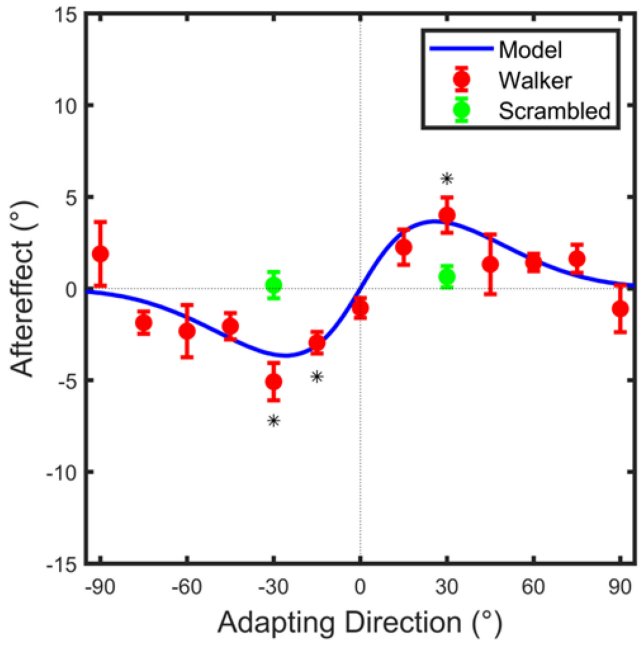

Note. Mean aftereffect as a function of the walking direction of the adaptor. The stimulus orientation perceived as walking directly toward the observer was estimated by finding the point of subjective equality (PSE) between walking directions that the participant judged as leftward versus rightward. Aftereffects are reported as the difference in the PSE between the baseline and the adapted state. The red and green dots represent aftereffects under walker and scrambled conditions, respectively. The error bars represent ±1 *SE* of the mean across participants for each adapting direction. The curved line shows the best fit of the model fitted to the response data. See the online article for the color version of this figure.
The * indicates adapting directions for which the mean aftereffect is significantly different from zero (* significance was determined by a Holm–Bonferroni adjusted alpha threshold).

that a shift in the PSE toward the side of the adapting stimulus is consistent with a repulsive perceptual aftereffect (e.g., a shift in the PSE toward the left indicates that test stimuli walking toward the left are now more likely to be perceived as walking directly toward the observer). As can be seen in Figure 4, symmetrical repulsive aftereffects were observed around the test direction (0°) with peak magnitude at $\pm 30°$ while the magnitude of aftereffects in the scrambled condition was close to zero. The observed pattern of data indicates that the effect of adaptation on perceived walking direction is tuned to the specific walking direction adapted to.

Statistical Analysis

A one-way repeated-measures ANOVA performed on the aftereffect data confirmed a significant main effect of adapting direction, $F\ (2,\ 16) = 7.60$, $p = .004$, $\eta_p^2 = 0.520$. Further one-sample *t*-tests were performed for each adapting direction, to establish for which directions the aftereffect was significantly different from zero. Significance for one-sample *t*-tests was determined by comparing each *p* value to an alpha threshold that was adjusted using the Holm–Bonferroni method. The results showed a significant effect for 3 of the 13 adapting directions: −30°, $t\ (7) = -4.99$, $p = .002$, Cohen's $d = 1.76$; −15°, $t\ (7) = -5.02$, $p = .002$, Cohen's $d = 1.77$; 30°, $t\ (7) = 4.16$, $p = .004$, Cohen's $d = 1.47$. The tuning of perceptual aftereffects across test directions provides insight into the underlying sensory coding of walking direction: discussed above in the section Psychophysical Modeling for Experiments 1 and 2.

Two paired samples *t*-tests were performed to compare the aftereffect between walker and scrambled stimulus for the $\pm 30°$ adapting directions, with results showing a significantly stronger repulsive aftereffect following adaptation to the walkers compared to the scrambled stimulus for both directions (significance was determined by a Holm–Bonferroni adjusted alpha threshold): for +30° (rightward), Walker versus Scrambled (mean difference = 3.36°), $t(7) = 4.55$, $p = .003$, Cohen's $d = 1.49$; for −30° (leftward), Walker versus Scrambled (mean difference = −5.26°), $t(7) = -4.17$, $p = .004$, Cohen's $d = 2.11$. Further one-sample *t*-tests were performed for each adapting direction under the scrambled condition to test whether the magnitude of aftereffects following exposure to a scrambled walker differed significantly from zero. Significance for one-sample *t*-tests was determined by a Holm–Bonferroni adjusted alpha threshold. The result revealed no significant effects of adaptation to scrambled walkers on the perceived walking direction of intact walkers: −30° condition, $t\ (7) = 0.258$, $p = .804$, Cohen's $d = .092$; 30° condition, $t\ (7) = 1.11$, $p = .306$, Cohen's $d = 0.390$. These results confirm that adaptation to walking direction relies on the holistic processing of the walker, rather than on the trajectories of the individual dots alone.

Model Fit

The psychophysical model of perceived walking direction was fit to the mean aftereffect across adapting directions. The fit between model predictions and response data is shown in Figure 4. The best-fitting parameters are $\sigma = 31.3°$ and $\alpha = 0.17$ (describing the width of the excitatory response and strength of adaptation, respectively), explaining 80.5% of the total variance. Qualitative aspects of the model predictions are consistent with the experimental data. Specifically, the peak aftereffects occur symmetrically on either side of the test direction and the magnitude of aftereffects tends to approach zero as adapting direction becomes increasingly averted beyond these two points. The resulting data show that a population-coding model of perceived walking direction can account well for the specific tuning of perceptual aftereffects, providing evidence that walking direction is coded in the relative activity across a neuronal population of direction-tuned units.

Experiment 2: Tuning of Aftereffects Across Different Test Walking Directions

Experiment 2 was designed to measure the tuning of perceptual aftereffects across changes in the walking direction of the test stimulus. Participants reported the walking direction of point-light walkers that varied in horizontal walking angle, and we measured how the perceived walking direction for a range of test stimuli changed as a result of adaptation.

Method

Participants

Eight participants (four males, four females), including four naïve participants and the four authors, took part in Experiment 2. The total test time for each participant was about 2 hr.

Apparatus and Stimuli

The stimuli we used in Experiment 2 were the same as in Experiment 1 but presented stereoscopically using a 3D monitor. The stimuli were presented stereoscopically because there were some "flipped" experiences (whereby walking direction toward the viewer was perceived as away from the viewer) reported during piloting for the wider test angles used in Experiment 2. All 3D stimuli were generated in MATLAB using Psychtoolbox with a binocular disparity of 6° of visual angle. The stimuli were presented on a 19-in. True3Di stereoscopic monitor (Redrover, Seoul, Republic of Korea) with a refresh rate of 60 Hz and pixel resolution of 1,680 × 1,050. Participants viewed the monitor through a pair of linearly polarizing filters, such that each eye received a different image from corresponding regions of visual space. The addition of binocular disparity cues made the point-light stimuli appear vividly three dimensional.

The response method was different from that in Experiment 1. Participants responded by using a mouse to rotate a spherical on-screen pointer (Figure 5A) in the horizontal plane between −90° (leftward) and +90° (rightward) to indicate the perceived walking direction of the test stimulus, allowing us to measure the perceived walking direction of test stimuli over a wide range of directions. The initial position of the pointer in each trial was randomized within the ratable range.

Experimental Design

Each participant completed three conditions in a randomized order. In each condition, the effects of adapting to a specific walking direction were tested across a range of test directions. Each condition consisted of a baseline phase followed by an adaptation phase. The adapting directions were −30°, 0°, and +30°. Directions of $\pm 30°$ were chosen as they produced the largest adaptation effects in

Figure 5

Illustration of Response Method and Results of Mean Aftereffect in Experiment 2

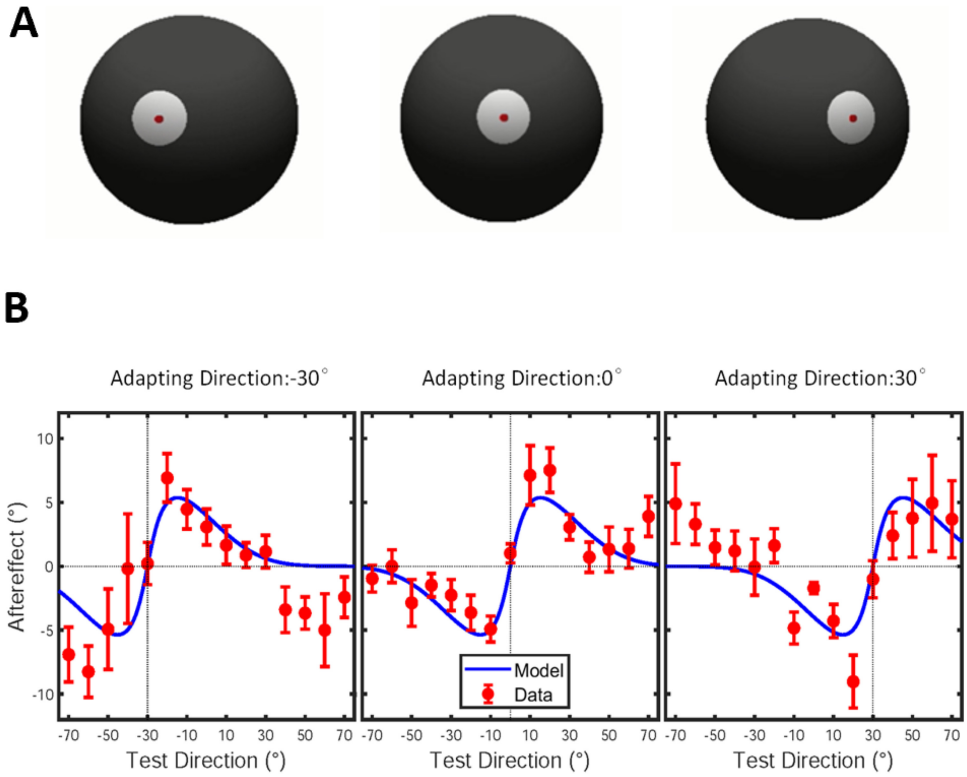

Note. (A) Participants reported the perceived walking direction of the point-light walker stimuli by rotating an on-screen pointer in Experiment 2. (B) Perceptual aftereffects following adaptation to walking direction differ in magnitude depending on the walking direction of the test stimulus. Data from Experiment 2 averaged across participants ($N = 8$) are shown. Averaged aftereffect as a function of test direction following adaptation to a walking direction of −30° (left), 0° (middle), and 30° (right). The error bars represent ±1 *SE* of the mean across participants for each test direction. The curved lines show the psychophysical model of perceived walking direction fitted to the response data. See the online article for the color version of this figure.

Experiment 1. At least a 10-min gap was left between the end of the adaptation phase of one condition and the beginning of the baseline phase of the next condition.

Each session began with a baseline phase. In each trial, the test walker stimuli were presented for 500 ms, followed by the presentation of the 3D pointer in the center of the screen to record the participant's response. If no response was made within 4 s, then the next trial would commence and the missed trial would be repeated at the end of the block (the average number of missed trials across participants was 2.13 out of a total of 1,080 trials per participant). A fixation point was presented for 1 s at the end of each trial before the next trial was initiated. The test stimuli ranged in the walking direction from −70° (leftward) to +70° (rightward) in 10° intervals (for a total of 15 test directions).

After each baseline phase, participants completed an adaptation phase. The adapting stimulus protocol was the same as in Experiment 1, except that the computer produced a short beep upon onset of each test stimulus and, as in the baseline phase, responses were made using the pointer to indicate the perceived walking direction of the test stimulus. Each test direction was tested 12 times in a pseudorandom order in each phase, such that each phase contained 180 trials in two blocks of 90 trials. Participants were provided with the opportunity to take a break after each block.

Results

Overview of Data

Experiment 2 investigated aftereffect magnitude as a function of test direction for three different adapting directions. The results are summarized in Figure 5B, showing the mean aftereffect across participants ($N = 8$) as a function of test direction for adapting directions of −30° (leftward), 0° (direct), and 30° (rightward), respectively. The aftereffect was computed as the difference in pointer response between baseline and adapted conditions. As can be seen most clearly in the middle panel of Figure 5B, the magnitude of aftereffects across test directions tends to be symmetrical around the adapting direction. Figure 5B shows a clear trend for the aftereffect to be repulsive, such that the perceived walking direction is biased away from the adapting direction, and the aftereffect tends to vary in magnitude depending on the difference between adapting and test directions.

Statistical Analysis

A two-way repeated-measures ANOVA was performed on the measured aftereffects. One factor was adapting direction (−30°, 0°, and 30°), and the other factor was the test direction relative to the adaptor, which ranged between −40° and +40° in 10° intervals. The effect of adaptation on perceived walking direction varied depending on the difference between adapting and test directions. This was reflected in a significant main effect of test direction relative to adaptor, $F(3, 19) = 21.8$, $p = 3 \times 10^{-6}$, $\eta_p^2 = 0.757$, as can be seen in Figure 5B, the aftereffects go in opposite directions either side of the adaptor (local repulsion) and with stronger magnitude for test directions closer to the adaptor. The main effect of adapting direction was not significant, $F(2, 14) = 0.414$, $p = .669$, $\eta_p^2 = .056$, nor was the interaction between test direction relative to adaptor and adapting direction, $F(3, 20) = 2.05$, $p = .142$, $\eta_p^2 = 0.227$. These results confirm what we have observed in the plots that adapting to −30°, 0°, and 30° produces clearly different patterns of effects; however, these different adapting directions produce a similar pattern of effects when test directions are considered relative to the position of the adaptor.

Model Fit

The model fit to the data from Experiment 2 is illustrated in Figure 5B. The best-fitting parameters are $\sigma = 23.2°$ and $\alpha = 0.31$, accounting for 63.8% of the total variance. As shown in Figure 5B, despite the presence of some residual error, the model is still clearly capturing key qualitative features of our empirical data: (a) The pattern of repulsive aftereffects around the adapting direction is symmetrical (i.e., the tuning curve is odd symmetric), (b) There tends to be little effect of adaptation on test stimuli with the same walking direction as the adaptor, with peak effects for test stimuli with walking directions near to the adaptor and weaker effects for test stimuli with walking directions far away from the adaptor, (c) As the walking direction of the adaptor varies, the peak aftereffects tend to occur for test directions which have the same difference relative to the adaptor walking direction, and (d) The magnitude of aftereffects (amplitude of the tuning curve) is similar across the three adapting directions. Hence, the population-coding model of perceived walking direction can account well for tuning of perceptual aftereffects both across adaptor walking directions (Experiment 1) and test walking directions (Experiment 2).

Experiment 3: Comparison of the Effect of Adaptation on Walking Directions Toward and Away From the Observer

In Experiments 1 and 2, we investigated the perception and sensory coding of walking direction for stimuli that ranged between 90° left and 90° right of directly toward the observer. In ecological environments, the horizontal walking directions that we typically observe span 360°, encompassing situations when we observe another person walking away from us. Experiment 3 was designed to test for specificity in the coding of horizontal walking direction in depth (i.e., toward vs. away from the observer). Participants reported the walking direction of point-light walkers that varied both in horizontal walking angle (i.e., leftward or rightward relative to the observer) and in depth (toward or away from the observer). We tested whether the effects of adaptation to horizontal walking direction depended on there being consistency between the depth direction of the adapting and test stimuli. The logic of the design is that specificity in perceptual aftereffects between the depth direction of the adapting and test stimuli would provide evidence for dissociable mechanisms coding horizontal walking directions toward the observer versus away from the observer, while generalization of perceptual aftereffects to test stimuli with the opposite depth direction to the adaptor would provide evidence for mechanisms coding horizontal walking direction that are agnostic to the depth direction of the walker. Overall, the purpose is to provide insight into the sensory coding of walking direction across the full 360° range of horizontal walking directions that occur in ecological environments.

Method

Participants

The sample was eight participants (three males, five females), including two authors and six naïve subjects. The total test time for each participant was about 2 hr. Three other participants were tested but excluded based on the results of a pretest (described below).

Apparatus and Stimuli

Stimuli were presented stereoscopically using the same apparatus as in Experiment 2.

Experimental Design

The design was similar to Experiment 1 except that adapting directions of ±30° and ±150° (Figure 6A) were used and test stimuli in separate conditions could be walking in a range of directions either toward or away from the observer. Both for stimuli walking toward and away from the observer, the participant's task was to judge whether each stimulus was walking to their left or their right, and their responses were recorded to measure the PSE (as in Experiment 1). The PSE calculated with test stimuli walking toward the observer provided a measure of the veridical test direction perceived as walking directly toward the observer, while the PSE for test stimuli walking away from the observer provided a measure of the veridical test direction perceived as walking directly away from the observer. Experiment 3 had a 2 × 4 within-subject design with two independent variables: test direction (toward or away), and adapting direction (+30°, −30°, +150°, or −150°). The order of these eight conditions was randomized across participants. Each condition consisted of a baseline and adaptation phases, as in Experiment 1. Test stimulus duration was 267 ms. There was at least a 10-min gap between the end of the adaptation phase of each condition and the beginning of the baseline phase of the next condition.

Pretest

Given the known tendency for point-light walkers to be perceived as facing the observer (Theusner et al., 2011), a pretest was performed before the formal experiment to exclude participants who had a strong bias to perceive stimuli walking away from them as heading toward them (or vice versa). There were two phases (short- and long-duration tests) in the pretest aimed at testing the perception of toward/away

Figure 6

Illustration of Adapting Walking Directions and Results of Mean Aftereffect in Experiment 3

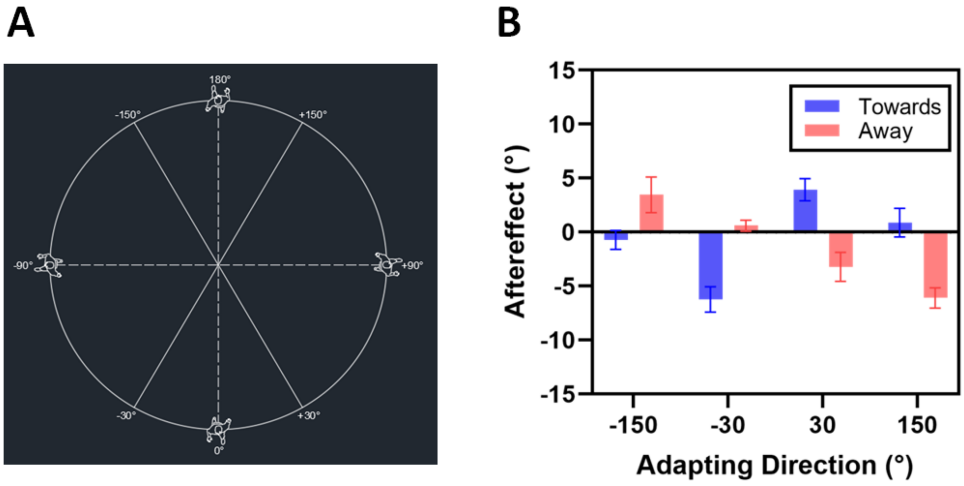

Note. (A) Illustration of the adaptor walking directions (±30° and ±150°) used in Experiment 3 from a bird's eye view. The directions with dashed lines (0°, ±90°, and 180°) are for reference (the walker figure was obtained from DesignsCAD; https://designscad.com/). (B) Data for Experiment 3, showing the aftereffect for adapting directions of ±30° and ±150° across different test directions (toward and away). Across conditions, we observed repulsive perceptual aftereffects, with the magnitude of the aftereffects greater when the depth direction of the adapting and test stimuli (toward vs. away) were consistent. For each participant, the aftereffect was calculated by subtracting the baseline point of subjective equalities (PSEs) from corresponding adapted PSEs. Error bars represent ±1 *SEM*. See the online article for the color version of this figure.

walking direction in conditions similar to the presentation of test and adapting stimuli, respectively, in Experiment 1. Participants were presented with a series of three-dimensional point-light walkers. In each trial of the short-duration test, a test stimulus was chosen at random from six test directions (±170°, ±10°, 0°, and 180°) and presented for 500 ms. Participants made their responses by pressing one of two buttons (down or up arrow) to indicate whether each walker was walking toward or away from them. In the long-duration test, the stimulus duration was 4 s and the test directions were ±150° and ±30°. Each direction was tested 20 times, resulting in 120 trials in the short-duration test and 80 trials in the long one. Participants were provided with the opportunity to take a break after completing half of the trials in each test phase. Participants with an accuracy of more than 90% in both the short- and long-duration tests were selected to proceed to the formal experiment.

Results

Overview of Data

Figure 6B shows how the effects of adaptation differ depending on whether the observer is adapted to stimuli walking toward them (−30° and 30°) or walking away from them (−150° and 150°). The aftereffect here was calculated by subtracting the unadapted PSEs from the corresponding adapted PSEs, such that for the test stimuli walking away from the observer, a positive aftereffect indicates an adapted PSE more leftward than the unadapted PSE; a negative aftereffect indicates an adapted PSE more rightward than the unadapted PSE. For test stimuli walking toward the observer, a positive aftereffect indicates an adapted PSE more rightward than the unadapted PSE; a negative aftereffect indicates an adapted PSE more leftward than the unadapted PSE. As can be seen, all the aftereffects tend to be repulsive regardless of the adapting or test directions. Importantly, Figure 6B also shows the aftereffects tend to be stronger when both adapting and testing on stimuli walking in the same direction (away from or toward the observer), rather than adapting on a stimulus walking away and testing on a stimulus walking toward (or vice versa).

Statistical Analysis

A two-way repeated-measures ANOVA was performed, with the test direction (toward and away) and adapting direction (30° and 150°) as the factors. The data used for the "adapting direction" factor were obtained by calculating the average repulsive effects of ±30° and ±150°, respectively, under different "test direction" conditions. The main effect of "test direction" was not significant, $F(1, 7) = 0.433$, $p = .531$, $\eta_p^2 = .058$; nor was the main effect of "adapting direction," $F(1, 7) = 2.31$, $p = .172$, $\eta_p^2 = 0.248$. Importantly, the interaction was highly significant, $F(1, 7) = 17.1$, $p = .004$, $\eta_p^2 = 0.710$. A Holm–Bonferroni corrected post hoc comparison showed that: for ±30° adaptors, the mean repulsive perceptual aftereffect was significantly stronger for test stimuli walking toward than away from the viewer (mean difference = 3.18°, $SD = 3.13°$, $t = 2.88$, $p = .024$, Cohen's $d = 1.77$); for ±150° adaptors, the mean repulsive perceptual aftereffect was significantly stronger for test stimuli walking away from than toward the viewer compared (mean difference = −3.98°, $SD = 2.85°$, $t = -3.95$, $p = .006$, Cohen's $d = 2.40$). Thus, the repulsive effect of adaptation on perceived walking direction depends on the consistency between the adapting direction relative to the test direction in three dimensions, which confirms the specificity of adaptation effects to whether the walking direction is toward or away from us. This

provides evidence that the horizontal direction in which a person is walking is coded using separable channels in our visual system when they are walking away from us compared to when they are walking toward us.

Experiment 4: Specificity of Adaptation to Biological Motion

In Experiments 1 and 2, we modeled how perceptual aftereffects following adaptation to walking direction could arise from selective changes in the sensitivity of a population of neurons each tuned to different preferred walking directions. Are these effects likely to reflect the operation of neurons tuned specifically to the direction of movement conveyed by the human form? While previous work indicates that adaptation to biological motion is unlikely to be explained by low-level adaptation in the visual system (e.g., because adaptation to walking direction persists across changes in the size and retinal position of the adapting and test stimuli; Jackson & Blake, 2010), these effects might in principle reflect adaptation of neurons tuned generally to object-level motion direction. Experiment 4 investigated the specificity of the walking-direction aftereffect to biological motion rather than more generic three-dimensional representations of motion direction.

Method

Participants

Eight participants (four males, four females) took part in Experiment 4, four of whom were the authors. Each of the other four had participated in one of the previous experiments. The total test time for each participant was about 2 hr.

Apparatus and Stimuli

To investigate the specificity of adaptation to walking direction, in addition to point-light walkers we added stereoscopic sphere stimuli which could be set to roll in any given direction. The sphere stimuli (Video 3 in the online supplemental material) were programmed and animated using MATLAB. Moreover, 200 dots were positioned randomly on the surface of a transparent sphere. Each dot had a Gaussian profile with sigma 1.2 pixels. To enhance the 3D perception of the sphere, the luminance of dots was different on the front and back surfaces: on the front, the luminance was 120 cd/m^2; on the back, it was 60 cd/m^2. The point-light walker stimuli were the same as in Experiments 2 and 3. We made the sphere diameter equal to the height of the walker and matched their effective translational speeds. All the stimuli in Experiment 4 (Figure 7A) were presented stereoscopically using the same apparatus as in Experiments 2 and 3.

Experimental Design

Experiment 4 had a $2 \times 2 \times 2$ within-subject design with three independent variables: adapting stimulus (sphere or walker), test stimulus (sphere or walker), and adapting direction ($-30°$ or $+30°$). The forced-choice task was to indicate the direction (left or right of directly toward the observer) in which each walker or sphere was heading by pressing one of two response buttons on the keyboard (left or right arrow). The dependent variable was the PSE (as used in Experiments 1 and 3) as a measure of the direction of the test for it to be perceived as heading directly toward the viewer. We divided the eight conditions into four pairs according to different adaptors (sphere toward $\pm 30°$ and walker toward $\pm 30°$) so that an interval to recover from adaptation was only needed after each pair of conditions rather than after every condition. To control for any build-up of adaptation effects within each pair of conditions, we alternated the order of test stimuli for each participant and counterbalanced them across participants. Other aspects of the design and procedure were exactly as in Experiment 3.

Results

Overview of Data

Experiment 4 investigated the specificity of adaptation to walking direction for biological motion, as opposed to more generic representations of motion direction. In particular, we tested whether adaptation to point-light walkers influenced the perceived direction of motion of a rolling sphere (and vice versa). The resulting data are shown in Figure 7B and 7C: the aftereffect is compared in different adapting and test conditions following adaptation to stimuli moving 30° left and 30° right of center. The aftereffect was calculated by subtracting the unadapted PSEs from the corresponding adapted PSEs. As can be seen in Figure 7B and 7C, aftereffects are greatest when the adapting and test stimuli are of the same category: in Figure 7B, when the test stimulus is a sphere, the sphere adaptors induce greater aftereffects than the walker adaptors; in Figure 7C, when the test stimulus is a walker, walker adaptors induce greater aftereffects than spheres.

Statistical Analysis

A two-way repeated-measures ANOVA was performed on the aftereffect data, with adapting stimulus (sphere or walker) and test stimulus (sphere or walker) as the factors. The data used for the "adapting stimulus" and "test stimulus" factors were obtained by calculating the average repulsive aftereffect between the adapting directions of $\pm 30°$ under each combination of the factors. Both main effects were significant: for adapting stimulus, $F\ (1,\ 7) = 28.3$, $p = .001$, $\eta_p^2 = 0.801$, and for test stimulus, $F\ (1,\ 7) = 24.7$, $p = .002$, $\eta_p^2 = 0.779$, indicating that sphere stimuli were both more potent as adaptors and more susceptible to adaptation as tests than walker stimuli. Importantly, there was a significant interaction between adapting and test stimulus directions, $F(1, 7) = 59.7$, $p = 1 \times 10^{-4}$, $\eta_p^2 = 0.895$. Post hoc analyses using the Holm–Bonferroni correction for significance showed that: for "walker" test stimuli, the aftereffect was significantly stronger when the adapting stimulus was a walker compared to when it was a sphere (mean difference $= 2.83°$, $SD = 2.30°$, $t = 3.47$, $p = .010$, Cohen's $d = 1.71$); for "sphere" test stimuli, the aftereffect was significantly stronger when the adapting stimulus was a sphere compared to when it was a walker (mean difference $= -8.31°$, $SD = 2.69°$, $t = -8.73$, $p = 5 \times 10^{-5}$, Cohen's $d = 4.50$), demonstrating the specificity of adaptation to walking direction: adaptors induce stronger aftereffects with tests within the same category.

Discussion

The present study investigated the neural mechanisms encoding perceived walking direction in the human visual system using an

Figure 7

Illustration of Experimental Conditions and Results of Mean Aftereffect in Experiment 4

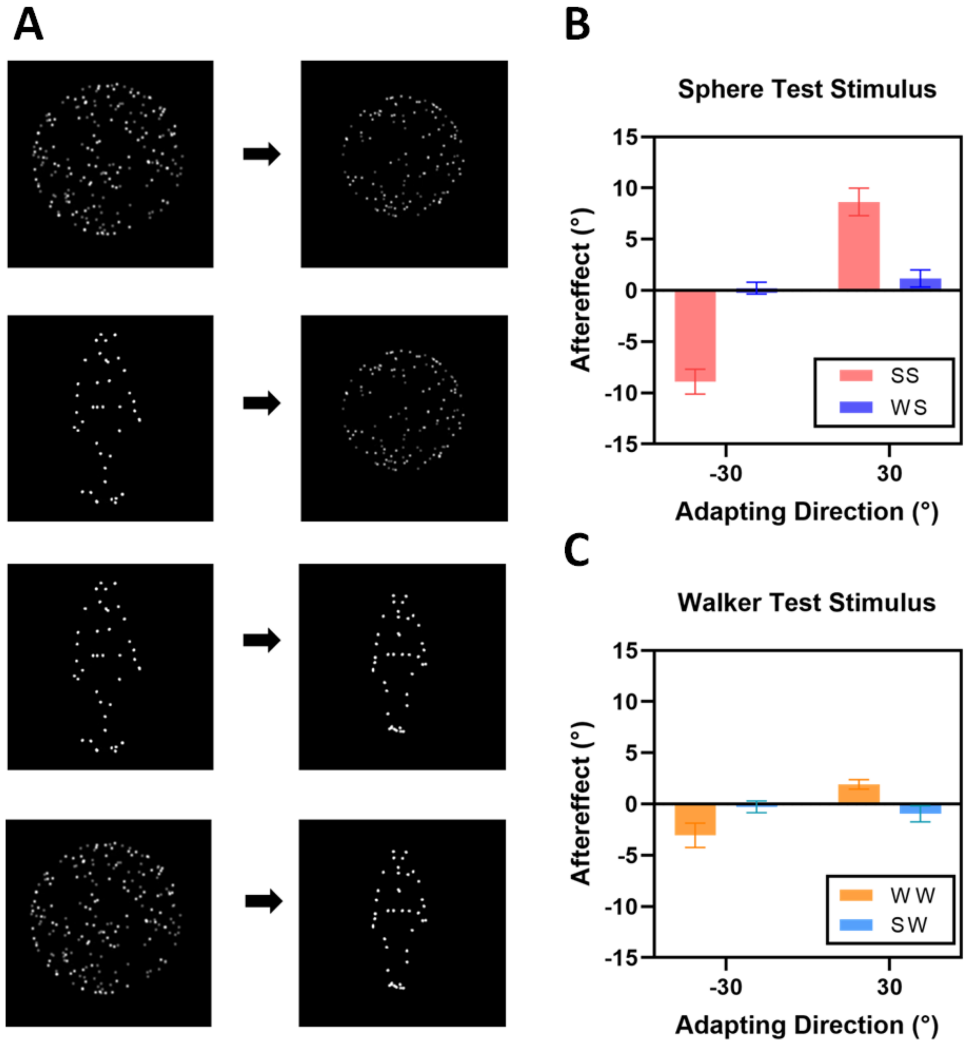

Note. (A) Illustration of different stimulus combinations. Left column denotes the adapting condition: walker or sphere (with adapting direction of +30° or −30°). Right column represents the test stimuli: walker or sphere. (B), (C) Specificity of adaptation to walking direction (Experiment 4). The aftereffect for adapting directions of +30° and −30° in different adapting conditions is shown (B) when the test stimulus was a sphere, (C) when the test stimulus was a walker. Error bars represent ±1 *SEM*. "SS" represents sphere adaptors followed by sphere test stimuli; "WS" represents walker adaptors followed by sphere test stimuli; "WW" represents walker adaptors followed by walker test stimuli; "SW" represents sphere adaptors followed by walker test stimuli. See the online article for the color version of this figure.

adaptation technique. In Experiment 1, we compared the magnitude of perceptual aftereffects across a range of adapting walking directions. Peak aftereffects appeared symmetrically following adaptation to walking directions averted by 30° either left or right of a direct test direction (Figure 4). In Experiment 2, we found that the magnitude of perceptual aftereffects following adaptation to walking direction depends on the walking direction of the test stimulus relative to the adaptor. In particular, we observed local repulsion of walking direction on either side of the adapted direction (Figure 5B). In Experiment 3, we measured whether the effects of adaptation differed as the adapting stimuli headed toward or away from the observers in specific walking directions of ±30° and ±150°. Repulsive aftereffects of a similar magnitude were observed for adaptor-test angular differences of ±30° regardless of whether motion was toward or away from the observer. However, for adaptor-test angular differences of ±150° (i.e., adaptor toward and test away, or vice versa) aftereffect magnitude was significantly reduced. In Experiment 4, we explored the specificity of adaptation to different categories of stimulus (walker and sphere). We tested whether adaptation to point-light walkers influenced the perceived direction of motion of a rolling sphere (and vice versa). The results show that aftereffects were strongest when adapting and test stimuli

belonged to the same category of 3D motion (human walker or rolling sphere) compared to when the category differed between the adapting and test stimuli.

Population Coding of Walking Direction

The tuning of perceptual aftereffects in Experiments 1 and 2 fits well with that predicted by a population-coding model, in which perceived walking direction is coded in terms of the relative activity across a population of direction-selective neurons with bell-shaped tuning profiles. The specific tuning of perceptual aftereffects that we observed also speaks to the bandwidth of the direction-selective channels. We can use the best-fitting values of the parameter, "σ," in the model (31.3° in Experiment 1 and 23.2° in Experiment 2) to estimate the minimum number of such channels that would be needed to span the full 360° range of horizontal walking directions. The best-fitting σ values correspond to a channel bandwidth of approximately 60° full width at half height. Assuming equally spaced channels overlapping at half height, six channels would then be required to span the full 360° range.

The population-coding model that we implement here to explain the tuning of adaptation to walking direction is comparable to models of the sensory coding of orientation in primary visual cortex or low-level motion direction (Suzuki et al., 2005). However, this coding scheme contrasts with the mechanisms implicated in some other aspects of high-level vision, including the coding of gaze direction (Palmer & Clifford, 2017), another essential social cue in primates. While adaptation to gaze direction is also associated with repulsive perceptual aftereffects, it exhibits notably different tuning to that which we observe for walking direction in the current study. In particular, adaptation to direct gaze generates notably weaker aftereffects than those measured for leftward or rightward averted gaze (Palmer & Clifford, 2017), unlike the similarity in amplitude and shape of the tuning profiles observed for different adapting directions in the current study (Experiment 2). The tuning of perceptual aftereffects following adaptation to horizontal gaze direction appears better accounted for by three sensory channels tuned broadly to left, right, and direct gaze direction (Calder et al., 2008; Palmer & Clifford, 2017), whereas the results of the present study indicate a larger bank of channels tuned across the full 360° range of walking directions.

Where in the brain might the population coding of walking direction be localized? Neurophysiological studies have identified the superior temporal sulcus (STS) as the principal brain region involved in coding social vision (Allison et al., 2000). There is converging evidence from single-cell recording studies in the macaque cortex that STS is responsible for the visual processing of high-level social attributes, such as gaze direction (Perrett et al., 1992), walking actions (Barraclough et al., 2006), and walking direction (Jellema et al., 2004). Specifically, Jellema et al. (2004) found cells in macaque STS that are sensitive to the walking direction of a person that the monkey is viewing. Neuroimaging studies (e.g., fMRI) in humans have also revealed that the posterior superior temporal sulcus (pSTS) processes biological motion (Jastorff & Orban, 2009). Consistent results have been found in humans using functional magnetic resonance adaptation (fMR–A) paradigms (Grill-Spector & Malach, 2001), such that human pSTS shows selectivity to high-level actions conveyed by biological motion (e.g., walking, running; Grossman et al., 2010; Thurman et al., 2016). The model we propose here speaks to the functional architecture of biological motion processing in terms of the computations involved but is agnostic as to the specific neural locus. Based on fits to our behavioral experimental data, the model makes testable predictions regarding for example the direction bandwidth of neurons involved in the coding of biological motion. Future research could use fMR–A to localize and further characterize the mechanisms underlying adaptation to walking direction in the human brain.

Coding Walking Direction in Depth

Experiment 3 provides evidence that the horizontal direction in which a person is walking is coded using separable mechanisms in our visual system when they are walking toward us compared to when they are walking away from us. These results complement previous findings that adaptation to a stimulus walking toward the observer can bias the perception of a bistable stimulus to be walking away from the observer, and vice versa (Jackson & Blake, 2010) and that aftereffects can be contingent on whether walking is forward or reversed (Benton et al, 2016). Taken together, the perceptual aftereffects measured in Experiments 1–3 and in these previous experiments describe an integrated system representing horizontal walking direction both left/right and in depth.

During piloting for Experiment 2, some participants tended to perceive a 2D figure walking toward them to be walking away, or vice versa. This led us to present the stimuli in 3D (i.e., stereoscopically), and this extra depth information provided by binocular disparities helped participants identify walking direction in depth more reliably (see also Bülthoff et al., 1998; Jackson & Blake, 2010). The depth reversals experienced by our observers when viewing 2D stimuli were interindividually variable and sometimes contrary to the facing bias reported in previous studies (Theusner et al., 2011; Vanrie et al., 2004). An explanation for such a facing bias from the view of error management theory (Haselton & Buss, 2000) relates to how human judgments and decision making under uncertainty tend to be biased toward the option that would be less costly were it an error (Clifford et al., 2015). As such, people may tend to adopt a "better safe than sorry" heuristic to avoid missing situations that pose a potential threat to them. In the context of a facing bias in perceived walking direction, this might be understood in terms of it being more socially relevant to detect someone walking toward you rather than away from you, or costlier to ignore someone walking toward you. It remains a question for future work to reveal the mechanism of this phenomenon.

Specificity of Adaptation to Biological Motion

The data from Experiment 4 provide evidence that the perceptual aftereffects that we measure across experiments reflect the adaptation of specific representations of walking direction for biological motion, as opposed to more generic representations of 3D motion direction. In future studies, it would be particularly interesting to examine how adaptation transfers between walking direction and other social signals, such as gaze direction or head orientation, which do not themselves require motion, but can serve a similar function of conveying the direction of attention and intentions of other people.

Local Versus Global Cues to Walking Direction

An ongoing debate in the field of biological motion perception concerns the relative contribution of local and global visual

processing. There are at least two ways in which the local versus global distinction is relevant in the context of adaptation to biological motion. One is the question of whether adaptation is occurring at the level of *spatially localized* motion detectors, such as neurons that respond to motion direction within a relatively small retinotopic receptive field. In the current study, we included a size change between the adapting and test stimuli to disrupt local spatial correspondences between motion signals in the adapting and test stimuli to minimize local motion adaptation and thus isolate adaptation to the walking direction at a more spatially generalized level of representation. The perceptual aftereffects that we observe across experiments are thus "high-level" in the sense that they are not tied closely to the retinotopic position in the way that occurs in the early visual processing of motion signals. This accords with previous research that has shown that perceptual aftereffects following adaptation to walking direction are robust to changes in size and retinal position of the test stimulus (Jackson & Blake, 2010).

The other question is whether judgments of walker direction are based on local elements of the stimulus, such as the specific motion trajectories of the hips or the feet, or on a more holistic representation of body motion. Both of these features are thought to play a role in biological motion perception, with some previous findings emphasizing the global processing of body motion (e.g., Beintema et al., 2006) and other findings highlighting the importance of local cues (e.g., Troje & Westhoff, 2006). For example, Troje and Westhoff (2006) find that the walking direction of a point-light walker (leftward vs. rightward) can still be determined following randomization of the dot locations (spatial scrambling) or of the phase of individual dot motions (temporal scrambling), indicating that the trajectories of individual dots are sufficient to provide some information about walking direction. Their results indicated that the local motion of the "feet" in particular helped to convey walking direction. In the current study, to address whether adaptation to walker direction is based on local elements of the stimulus or on a more holistic representation of body motion, we implemented a control adapting stimulus in which the spatial location and temporal phase of the dots were scrambled to disrupt holistic structure while maintaining the trajectories of local elements. Any aftereffects that occurred following adaptation to this scrambled control stimulus would be attributable to adaptation based on the motion of local elements, while increased adaptation to an intact walker relative to the control would indicate adaptation based on a more holistic representation. The significant difference we found in repulsive aftereffects between intact walkers and scrambled walkers suggests that adaptation to walking direction occurred at a global level, relying on the sense of walking direction conveyed by the spatiotemporal configuration of visual features. Moreover, the nonsignificant effect we found in the scrambled condition constitutes a lack of evidence for adaptation to direction conveyed by "local" bodily cues.

Conclusion

To conclude, our study provides further evidence for and characterization of neural mechanisms in the human visual system tuned to specific walking directions. We measured repulsive aftereffects of adaptation to biological motion whose magnitude depends on the difference between adapting and test directions. We implemented a simple functional model of walking direction to examine how information is coded across a neuronal population and found that a multichannel coding model can well explain the specific tuning profiles observed, thus providing a framework for future computational work to explore other aspects of the processing of biological motion. Our study also provides a foundation for investigating the adaptive sensory coding of walking direction in clinical populations that can exhibit differences in sensitivity to nonverbal social cues, such as autism and schizophrenia.

References

Allison, T., Puce, A., & McCarthy, G. (2000). Social perception from visual cues: Role of the STS region. *Trends in Cognitive Sciences*, *4*(7), 267–278. https://doi.org/10.1016/S1364-6613(00)01501-1

Barraclough, N. E., Xiao, D., Oram, M. W., & Perrett, D. I. (2006). The sensitivity of primate STS neurons to walking sequences and to the degree of articulation in static images. *Progress in Brain Research*, *154*(Part A), 135–148. https://doi.org/10.1016/S0079-6123(06)54007-5

Beintema, J. A., Georg, K., & Lappe, M. (2006). Perception of biological motion from limited-lifetime stimuli. *Perception & Psychophysics*, *68*(4), 613–624. https://doi.org/10.3758/bf03208763

Benton, C. P., Thirkettle, M., & Scott-Samuel, N. E. (2016). Biological movement and the encoding of its motion and orientation. *Scientific Reports*, *6*(1), Article 22393. https://doi.org/10.1038/srep22393

Bertenthal, B. I., & Pinto, J. (1994). Global processing of biological motions. *Psychological Science*, *5*(4), 221–225. https://doi.org/10.1111/j.1467-9280.1994.tb00504.x

Blake, R., & Shiffrar, M. (2007). Perception of human motion. *Annual Review of Psychology*, *58*(1), 47–73. https://doi.org/10.1146/annurev.psych.57.102904.190152

Brainard, D. H. (1997). The psychophysics toolbox. *Spatial Vision*, *10*(4), 433–436. https://doi.org/10.1163/156856897X00357

Bülthoff, I., Bülthoff, H., & Sinha, P. (1998). Top-down influences on stereoscopic depth-perception. *Nature Neuroscience*, *1*(3), 254–257. https://doi.org/10.1038/699

Calder, A. J., Jenkins, R., Cassel, A., & Clifford, C. W. (2008). Visual representation of eye gaze is coded by a nonopponent multichannel system. *Journal of Experimental Psychology: General*, *137*(2), 244–261. https://doi.org/10.1037/0096-3445.137.2.244

Carandini, M., & Heeger, D. J. (2012). Normalization as a canonical neural computation. *Nature Reviews Neuroscience*, *13*(1), 51–62. https://doi.org/10.1038/nrn3136

Chen, C., Boyce, W. P., Palmer, C. J., & Clifford, C. W. (2023). Adaptation to walking direction in biological motion [Data set]. https://osf.io/t8cdn/?view_only=4e3f19ba1060462995c1d5dbd5807bde

Clifford, C. W. G., Mareschal, I., Otsuka, Y., & Watson, T. L. (2015). A Bayesian approach to person perception. *Consciousness and Cognition*, *36*, 406–413. https://doi.org/10.1016/j.concog.2015.03.015

Clifford, C. W. G., & Rhodes, G. (2005). *Fitting the mind to the world: Adaptation and after-effects in high-level vision* (Vol. 2). Oxford University Press.

Clifford, C. W. G., Webster, M. A., Stanley, G. B., Stocker, A. A., Kohn, A., Sharpee, T. O., & Schwartz, O. (2007). Visual adaptation: Neural, psychological and computational aspects. *Vision Research*, *47*(25), 3125–3131. https://doi.org/10.1016/j.visres.2007.08.023

Clifford, C. W. G., Wenderoth, P., & Spehar, B. (2000). A functional angle on some after-effects in cortical vision. *Proceedings of the Royal Society of London. Series B: Biological Sciences*, *267*(1454), 1705–1710. https://doi.org/10.1098/rspb.2000.1198

Cutting, J. E., & Kozlowski, L. T. (1977). Recognizing friends by their walk: Gait perception without familiarity cues. *Bulletin of the Psychonomic Society*, *9*(5), 353–356. https://doi.org/10.3758/BF03337021

Dittrich, W. H., Troscianko, T., Lea, S. E., & Morgan, D. (1996). Perception of emotion from dynamic point-light displays represented in dance. *Perception*, *25*(6), 727–738. https://doi.org/10.1068/p250727

Frisby, J. P., & Stone, J. V. (2010). *Seeing: The computational approach to biological vision*. MIT Press.

Grill-Spector, K., & Malach, R. (2001). fMR-adaptation: A tool for studying the functional properties of human cortical neurons. *Acta Psychologica*, *107*(1–3), 293–321. https://doi.org/10.1016/S0001-6918(01)00019-1

Grossman, E. D., Jardine, N. L., & Pyles, J. A. (2010). fMR-adaptation reveals invariant coding of biological motion on the human STS. *Frontiers in Human Neuroscience*, *4*(5), 15. https://doi.org/10.3389/neuro.09.015.2010

Haselton, M. G., & Buss, D. M. (2000). Error management theory: A new perspective on biases in cross-sex mind reading. *Journal of Personality and Social Psychology*, *78*(1), 81–91. https://doi.org/10.1037/0022-3514.78.1.81

Heeger, D. J. (1992). Normalization of cell responses in cat striate cortex. *Visual Neuroscience*, *9*(2), 181–197. https://doi.org/10.1017/S0952523800009640

Jackson, S., & Blake, R. (2010). Neural integration of information specifying human structure from form, motion, and depth. *The Journal of Neuroscience*, *30*(3), 838–848. https://doi.org/10.1523/JNEUROSCI.3116-09.2010

Jastorff, J., & Orban, G. A. (2009). Human functional magnetic resonance imaging reveals separation and integration of shape and motion cues in biological motion processing. *The Journal of Neuroscience*, *29*(22), 7315–7329. https://doi.org/10.1523/JNEUROSCI.4870-08.2009

Jellema, T., Maassen, G., & Perrett, D. I. (2004). Single cell integration of animate form, motion and location in the superior temporal cortex of the macaque monkey. *Cerebral Cortex*, *14*(7), 781–790. https://doi.org/10.1093/cercor/bhh038

Jenkins, R., Beaver, J. D., & Calder, A. J. (2006). I thought you were looking at me: Direction-specific aftereffects in gaze perception. *Psychological Science*, *17*(6), 506–513. https://doi.org/10.1111/j.1467-9280.2006.01736.x

Jiang, Y., & He, S. (2008). Neural encoding of walking direction in biological motion: Evidence from direction-specific adaptation and functional neuroimaging. *Journal of Vision*, *8*(6), Article 902. https://doi.org/10.1167/8.6.902

Johansson, G. (1973). Visual perception of biological motion and a model for its analysis. *Perception & Psychophysics*, *14*(2), 201–211. https://doi.org/10.3758/BF03212378

Jordan, H., Fallah, M., & Stoner, G. R. (2006). Adaptation of gender derived from biological motion. *Nature Neuroscience*, *9*(6), 738–739. https://doi.org/10.1038/nn1710

Kontsevich, L. L., & Tyler, C. W. (1999). Bayesian Adaptive estimation of psychometric slope and threshold. *Vision Research*, *39*(16), 2729–2737. https://doi.org/10.1016/S0042-6989(98)00285-5

Leopold, D. A., O'Toole, A. J., Vetter, T., & Blanz, V. (2001). Prototype-referenced shape encoding revealed by high-level aftereffects. *Nature Neuroscience*, *4*(1), 89–94. https://doi.org/10.1038/82947

Mather, G., Pavan, A., Campana, G., & Casco, C. (2008). The motion aftereffect reloaded. *Trends in Cognitive Sciences*, *12*(12), 481–487. https://doi.org/10.1016/j.tics.2008.09.002

Montepare, J. M., Goldstein, S. B., & Clausen, A. (1987). The identification of emotions from gait information. *Journal of Nonverbal Behavior*, *11*(1), 33–42. https://doi.org/10.1007/BF00999605

Neri, P., Morrone, M. C., & Burr, D. C. (1998). Seeing biological motion. *Nature*, *395*(6705), 894–896. https://doi.org/10.1038/27661

Palmer, C. J., & Clifford, C. W. (2017). Functional mechanisms encoding others' direction of gaze in the human nervous system. *Journal of Cognitive Neuroscience*, *29*(10), 1725–1738. https://doi.org/10.1162/jocn_a_01150

Perrett, D. I., Hietanen, J. K., Oram, M. W., & Benson, P. J. (1992). Organization and functions of cells responsive to faces in the temporal cortex. *Philosophical Transactions of the Royal Society of London. Series B: Biological Sciences*, *335*(1273), 23–30. https://doi.org/10.1098/rstb.1992.0003

Pollick, F. E., Kay, J. W., Heim, K., & Stringer, R. (2005). Gender recognition from point-light walkers. *Journal of Experimental Psychology: Human Perception and Performance*, *31*(6), 1247–1265. https://doi.org/10.1037/0096-1523.31.6.1247

Suzuki, S., Clifford, C., & Rhodes, G. (2005). High-level pattern coding revealed by brief shape aftereffects. In C. A. Heywood, & G. M. Innocenti (Eds.), *Fitting the mind to the world: Adaptation and aftereffects in high-level vision* (Vol. 2, pp. 135–172). Oxford University Press.

Theusner, S., de Lussanet, M. H. E., & Lappe, M. (2011). Adaptation to biological motion leads to a motion and a form aftereffect. *Attention, Perception, & Psychophysics*, *73*(6), 1843–1855. https://doi.org/10.3758/s13414-011-0133-7

Thompson, B., Hansen, B. C., Hess, R. F., & Troje, N. F. (2007). Peripheral vision: Good for biological motion, bad for signal noise segregation? *Journal of Vision*, *7*(10), Article 12. https://doi.org/10.1167/7.10.12

Thornton, I. M., Pinto, J., & Shiffrar, M. (1998). The visual perception of human locomotion. *Cognitive Neuropsychology*, *15*(6–8), 535–552. https://doi.org/10.1080/026432998381014

Thornton, I. M., & Vuong, Q. C. (2004). Incidental processing of biological motion. *Current Biology*, *14*(12), 1084–1089. https://doi.org/10.1016/j.cub.2004.06.025

Thurman, S. M., & Grossman, E. D. (2008). Temporal "Bubbles" reveal key features for point-light biological motion perception. *Journal of Vision*, *8*(3), Article 28. https://doi.org/10.1167/8.3.28

Thurman, S. M., van Boxtel, J. J. A., Monti, M. M., Chiang, J. N., & Lu, H. (2016). Neural adaptation in pSTS correlates with perceptual aftereffects to biological motion and with autistic traits. *Neuroimage*, *136*, 149–161. https://doi.org/10.1016/j.neuroimage.2016.05.015

Troje, N. F. (2002). Decomposing biological motion: A framework for analysis and synthesis of human gait patterns. *Journal of Vision*, *2*(5), Article 2. https://doi.org/10.1167/2.5.2

Troje, N. F., Sadr, J., Geyer, H., & Nakayama, K. (2006). Adaptation aftereffects in the perception of gender from biological motion. *Journal of Vision*, *6*(8), Article 7. https://doi.org/10.1167/6.8.7

Troje, N. F., & Westhoff, C. (2006). The inversion effect in biological motion perception: Evidence for a "life detector"? *Current Biology*, *16*(8), 821–824. https://doi.org/10.1016/j.cub.2006.03.022

Troje, N. F., Westhoff, C., & Lavrov, M. (2005). Person identification from biological motion: Effects of structural and kinematic cues. *Perception & Psychophysics*, *67*(4), 667–675. https://doi.org/10.3758/bf03193523

van Boxtel, J. J., & Lu, H. (2013). A biological motion toolbox for reading, displaying, and manipulating motion capture data in research settings. *Journal of Vision*, *13*(12), Article 7. https://doi.org/10.1167/13.12.7

Vanrie, J., Dekeyser, M., & Verfaillie, K. (2004). Bistability and biasing effects in the perception of ambiguous point-light walkers. *Perception*, *33*(5), 547–560. https://doi.org/10.1068/p5004

Watson, T. L., Pearson, J., & Clifford, C. W. (2004). Perceptual grouping of biological motion promotes binocular rivalry. *Current Biology*, *14*(18), 1670–1674. https://doi.org/10.1016/j.cub.2004.08.064

Received April 7, 2022
Revision received January 29, 2023
Accepted February 9, 2023 ■